Gluconeogenesis using glycerol as a substrate in bloodstream-form Trypanosoma brucei

Kovarova, Julie; Nagar, Rupa; Correia Faria, Joana; Ferguson, Michael; Barrett, Michael P.; Horn, David

Published in:
PLoS Pathogens

DOI:
10.1371/journal.ppat.1007475

Publication date:
2018

Licence:
CC BY

Document Version
Publisher's PDF, also known as Version of record

ORAL DISEASES
Leading in Oral, Maxillofacial, Head & Neck Medicine

Ultrastructural analysis of collagen fibril diameter distribution in cleft lip

Journal:	*Oral Diseases*
Manuscript ID	ODI-05-18-OM-6266.R1
Manuscript Type:	Original Manuscript
Date Submitted by the Author:	n/a
Complete List of Authors:	Khan , Mohammad Faisal ; University of Ferrara, Department of Biomedical and Specialty Surgical Sciences, Section of Medical Biochemistry, Molecular Biology and Genetics Little, Julian; University of Ottawa, School of Epidemiology, Public Health and Preventive Medicine Nag, Tapas; All India Institute of Medical Sciences, Department of Anatomy; All India Institute of Medical Sciences, Sophisticated Analytical Instrumentation Facility (SAIF), Department of Anatomy Mossey, PA; University of Dundee, Craniofacial Development at the World Health Organization–collaborating Centre for Oral and Craniofacial Research, Dental Hospital and School Autelitano, Luca; University of Milan, Smile House, Regional Centre for Orofacial Clefts and Craniofacial Anomalies, Department of Cranio-Maxillo-Facial Surgery, San Paolo Hospital Meazzini, Maria; University of Milan, Smile House, Regional Centre for Orofacial Clefts and Craniofacial Anomalies, Department of Cranio-Maxillo-Facial Surgery, San Paolo Hospital Merajuddin, Ahmed; King Saud University, Department of Pathology, College of Medicine Singh, Anuraag; All India Institute of Medical Sciences, Sophisticated Analytical Instrumentation Facility (SAIF), Department of Anatomy Rubini, Michele; University of Ferrara, Department of Biomedical and Specialty Surgical Sciences, Section of Medical Biochemistry, Molecular Biology and Genetics
Keywords:	cleft lip, cleft lip and palate, collagen fibrils-edge-diameter, collagen number density, fibril-area fraction, ImageJ

Title: Ultrastructural analysis of collagen fibril diameter distribution in cleft lip

Mohammad Faisal J Khan[1], Julian Little[2], Tapas Chandra Nag[3,7] , Peter Anthony Mossey[4], Luca Autelitano[5], Maria Costanza Meazzini[5], Ahmed Merajuddin[6], Anuraag Singh[7], Michele Rubini[1].

1. Department of Biomedical and Specialty Surgical Sciences, Section of Medical Biochemistry, Molecular Biology and Genetics, University of Ferrara, Ferrara, Italy.

2. School of Epidemiology and Public Health, University of Ottawa, Ottawa, Ontario, Canada.

3. Department of Anatomy, All India Institute of Medical Sciences, New Delhi, India.

4. Craniofacial Development at the World Health Organization–collaborating Centre for Oral and Craniofacial Research, Dental Hospital and School, University of Dundee, Dundee, Scotland.

5. Smile House, Regional Centre for Orofacial Clefts and Craniofacial Anomalies, Department of Cranio-Maxillo-Facial Surgery, San Paolo Hospital, University of Milan, Milan, Italy.

6. Department of Pathology, College of Medicine, King Saud University, Riyadh, Saudi Arabia.

7. Sophisticated Analytical Instrumentation Facility (SAIF), Department of Anatomy, All India Institute of Medical Sciences, New Delhi, India.

Corresponding author:

Mohammad Faisal Jamal Khan, Department of Biomedical and Specialty Surgical Sciences, Section of Medical Biochemistry, Molecular Biology and Genetics, University of Ferrara, Via Fossato di Mortara 74 I-44121, Ferrara, Italy. Fax No: +39.0532.236157 Email: khnmmm@unife.it

Key words: cleft lip, cleft lip and palate, collagen fibrils-edge-diameter, collagen number density, fibril-area fraction, ImageJ.

Running head: Collagen fibrils across two sides of a cleft lip.

Date of submission: May 28th, 2018

Ultrastructural analysis of collagen fibril diameter distribution in cleft lip

Abstract

Objective: A preliminary study to determine collagen fibril diameter (CF-ED) distribution on medial and lateral sides of cleft lip (CL).

Material and Methods: Tissue samples from medial and lateral sides of CL were fixed in 2.5% glutaraldehyde and 1% osmium tetroxide and embedded in Araldite CY212 resin for transmission electron microscopy. The analysis of CF-ED was ~~ere~~ performed using the ImageJ program. To characterize the packaging of collagen fibrils (CFs) in the two tissues, we estimated the collagen number density (CF-ND) and fibril-area-fraction (FAF). Differences in measurements across the two sides were calculated using Wilcoxon signed rank test.

Results: The CF-ED was statistically significantly ($p<0.001$) smaller on the medial side (45.69 ± 7.89 nm) than on the lateral side (54.18 ± 7.62 nm). The medial side had a higher CF-ND and a higher percentage of FAF than the lateral side.

Conclusion: Our finding of a smaller CF-ED and higher CF-ND and FAF for the medial side suggest possible differences in size and distribution of CFs between medial and lateral sides of CL. This finding provides knowledge towards underlying tissue biomechanics that may help reconstruction of perioral tissue scaffolds, ultimately resulting in better treatment of patients with oral clefts.

Introduction

Cleft lip with or without palate (CL/P) is one of the most frequent congenital anomalies worldwide, with a prevalence among live births of 1 in 700 (Dixon, Marazita, Beaty, & Murray, 2011). Approximately, 70-80% of CL/P cases are non-syndromic (Leslie et al., 2016). Labial architecture is dramatically altered in CL/P cases that may be attributed to the impairment in the muscle forces (Barlow, Trotman, Chu, & Lee, 2012; Trotman, Barlow, & Faraway, 2007). CL/P clinically can occur as a unilateral or bilateral gap between the medial and the lateral upper lip structures (Carroll & Mossey, 2012).

The development of the upper lip involves co-ordination among complex series of events which requires cell migration, differentiation and apoptosis (Mossey, Little, Munger, Dixon, & Shaw, 2009), and particularly growth and fusion of the paired medial nasal process (MNP) and maxillary process (MxP) (Jiang, Bush, & Lidral, 2006). The MNP and MxP form the medial and lateral aspects of the upper lip structure, respectively (Dixon et al., 2011). Any cellular and morphological changes affecting the growth or fusion of the MNP and/or MxP may result in orofacial clefting involving the upper lip (Walker & Podda, 2018).

A fine modulation in the extracellular matrix in the orofacial region during development is essential for the cells to interact and respond to the remodeling or change in mechanical properties of the extracellular matrix (McDaniel et al., 2007; Gagliano et al., 2010), which is likely critical to cellular migration, differentiation (Badylak, 2005), and etiology of orofacial cleft (Smane-Filipova, Pilmane, & Akota., 2016; Mansell et al., 2000). Studies in experimental models of fibroblast cells obtained from CL/P cases have suggested molecular mechanisms involved in phenotypic variation among fibroblasts (Bosi et al., 1999; Bodo et al., 1999). These mechanisms are thought to be regulated by the collagen degradation pathway via matrix metalloproteinases and their endogenous tissue inhibitors; or by regulation of collagen cross-linking (Gagliano et al., 2010). Mechanical loading of the tissues can influence metalloproteinases expression, production and activity causing an imbalance between metalloproteinases and their inhibitors that further remodel the tissue extracellular matrix component (Nagase, Visse, & Murphy, 2006). Relatively little attention has been given to the structure of the extracellular matrix in CL/P tissues.

The collagen fibrils (CFs) and proteoglycans are the two major components that make up the extracellular matrix of oral tissue structure (Levine, 2011), with fibrillar shaped collagen being the predominant component. This fibrillar collagens form a rope like structure, which shows characteristic banding pattern, and appears rounded on a transverse section under electron microscopy (Arseni et al., 2018). Several ultrastructural studies on healthy and

pathological oral connective tissues have been reported (Chavier, Couble, Magloire, & Grimaud, 1984; Pêgo et al., 2016; Agrawal, Rai, & Jain, 2011); these studies have shown different CF arrangement in different oral tissues, with variation in CF distribution pattern and fibril diameter (Craig, Birtles, Conway, & Parry, 1989; Xu, Ohsaki, Nagata, & Kurisu, 1993) and exposure to biomechanical forces (Craig, Eikenberry & Parry, 1987).

The few studies that have investigated the relationship between structural and biomechanical properties in clefting have generally focused on proteoglycans and their involvement in cleft palate (Brinkley & Morris-Wiman, 1987a), with evidence of hyaluronic acid proteoglycan content regulating the hydration, and allowing elevation of palatal shelves (Brinkley & Morris-Wiman, 1987b). However, knowledge of the variations in structural organization of CFs, which is pivotal in determining the biomechanical properties of the oral soft connective tissue (Cornelissen, Stoop, Von den Hoff, Maltha, & Kuijpers-Jagtman, 2000) has been little investigated in research on orofacial clefts, particularly CL.

The tensile strength of the extracellular matrix and the mass average diameter of the constituent CFs are positively correlated, with CF diameter reflecting the mechanical properties of a tissue (Parry, Barnes, & Craig, 1978). Tissues with small diameter CFs can withstand high mechanical load (Parry, 1988), determined by unimodality or bimodality-mainly represented in fibril frequency histogram (Williams, Elder, Horstemeyer, & Harbarger, 2008). Additional studies in a mouse model have showed the structural-functional relationship between CFs area fraction to be correlated to strength and stiffness of a tissue (Robinson, Lin, Jawad, Iozzo, & Soslowsky, 2004).

The size distribution of CFs is mainly determined by intra-fibrillar covalent cross-linking provided by enzymes of the Lysyl-oxidase (LOX) family (Herchenhan et al., 2015). The deletion of *LOXL3* gene has been shown to impair collagen assembly and cross-linking leading to smaller size CFs during palate development in a mouse model (Zhang et al., 2015). Additionally, our group has recently found a variant in this gene to be associated with non-syndromic cleft palate (Khan et al., 2018). The morphogenesis of lip and palate fusion involves highly regulated sharing of signaling molecules, and so it is possible that lip fusion promotes palate fusion (Smane-Filipova et al., 2016). Therefore, improper fusion of the lip may secondarily affect palate fusion (Meng, Bian, Torensma, & Von den Hoff, 2009). This inter-relationship demonstrates the importance of investigating CFs distribution to gain insight into the contribution of extracellular matrix component at a stage prior to palate development, i.e. upper lip fusion, which to our knowledge, remains largely unknown.

There are many approaches to studying the involvement of extracellular matrix in CL/P morphogenesis such as investigation of metalloproteinases and their inhibitors and collagen turnover, and/or the genes encoding them, as previously described. Each approach emphasizes different aspects of the extracellular matrix structure. However, to our knowledge no studies to date have investigated the organizational diversity of CFs, as revealed by electron microscopy, in medial and lateral tissues of CL cases. This might in future provide possible useful avenues underlying tissue biomechanics and help towards reconstruction of perioral tissue scaffolds.

Materials and Methods

Tissue samples

Tissue samples from the medial and lateral sides of CL were collected from four non-syndromic CL/P cases (two with CL and two with cleft lip and palate [CLP], each with the cleft on the left side). The average age of cases at the time of first lip surgery was eight months (95% CI 4.6-11.4). The samples were collected at the Regional Centre for Orofacial Clefts and Craniofacial Anomalies, San Paolo Hospital, Milan, Italy in the framework of the PENTACLEFT project (Khan et al., 2018), which was approved by local IRB (prot. N.08-2011). Written informed consent from one or both parents for case enrolment was obtained.

Tissue fixation and processing for transmission electron microscopy

The medial and lateral CL tissues were fixed in 2.5% glutaraldehyde in 0.1 M phosphate buffer at pH 7.4 overnight. They were then washed three times in 0.1 M phosphate-buffer (15 min ×3). Tissues were post-fixed in 1% osmium tetroxide for 1 hour, washed thrice (15 min ×3) with buffer and dehydrated with graded series of ethanol (50-100%) for 30 min in each. Tissues were infiltrated in toluene and Araldite CY212, and embedded in Araldite resin. Four blocks for each specimen (two for medial and two for lateral tissues) were prepared and polymerised in Araldite CY212 at 60°C for 72 hours. Ultrathin sections (70 nm thickness) were cut (from different regions of the tissues in the block) using Leica ultramicrotome UC7 and collected on 200 mesh copper grids. Each grid with ultrathin sections were stained with 2% uranyl acetate (10 min) and lead citrate (10 min), and then observed under Tecnai G^2-20 transmission electron microscope (FEI Company, The Netherlands) at an operative voltage of 200 kV, at the Sophisticated Analytical Instrumentation facility (SAIF)-Electron Microscope Facility, All India Institute of Medical Sciences (AIIMS), New Delhi, India.

Image acquisition and processing

The images were acquired under transmission electron microscope at 60000X using Digital Micrograph (Gatan, Inc.) software. Images were acquired for the medial and lateral sides of each CL specimen (with different levels of the blocks - each section being separated by a distance of 500 nm). The areas and diameter of CFs from each medial and lateral CL tissue specimen were measured using an open-source image processing software, ImageJ (Ver. ImageJ 1.49h, Dresden, Germany). Equating the irregular transverse area (A*i*) of the collagen fibrils to an equivalent circle, led to the determination of edge diameter of CFs ($ED = \sqrt{2\,Ai/\,3.142}$), as previously described (Khan, Nag, Igathinathane, Osuagwu & Rubini, 2015).

To analyse the collagen fibril diameter (CF-ED), our original 8-bit greyscale images were processed to obtain the binary image. Standard commands of ImageJ were used for preprocessing the images (Ferreira & Rasband, 2012). The original greyscale image (Figure 1a) was first segmented using thresholding image with moments scheme and no dark background (Figure 1b). The lower and the upper limit of intensities were then adjusted for clear visibility of CFs of interest, a lower threshold limit of 0 and upper limit of 120-170 for white background were found to be optimal for images to convert to binary format (Figure 1c). The sequence of assigned operations in ImageJ were followed for a section of input-image to obtain an area desired for each CFs which were color coded using ROI color coder plugin (Ferreira, 2014) for clear visualization of different CFs (Figure 1d-g). The output area of each CF was in pixel unit which made it essential to convert to physical unit by using the line tool of ImageJ. The data were transferred to Excel spreadsheet from ImageJ software for further analysis.

Collagen number density (CF-ND) and fibril-area-fraction (FAF)

Collagen number density is the number of CFs per unit area (μm^2). It was calculated using the formula; $ND = \frac{Total\ CF\ number}{Total\ image\ area\ (\mu m2)}$

We made use of the A*i* of each of the CF included within an image area (A) to calculate the fibril-area-fraction also known as fibril-volume fraction (Starborg et al., 2013) by making use of the formula; $FAF = \sum \frac{Ai}{A}$ (A*i*; transverse area of each fibril and A; is the total area of an image).

Statistical analysis

The distribution of collagen fibrils were checked for normality using Shapiro–Wilk test for small samples in the IBM SPSS Statistics 21. The differences in measurements of CF-ED across the medial and lateral sides of CL was done using Wilcoxon signed rank test. In addition a paired student's *t*-test was used to check for differences in FAF and CF-ND between medial and lateral tissues. Considering the total of four cases included in this study, and assuming an α-error (two-tailed) of 0.05 and a 1-β-error of 0.80, at least 208 CF-ED from each side per sample would be required to detect a change of 20% in CF-ED, FAF or CF-ND, as calculated using G * POWER software 3.1.9.2 version (Faul, Erdfelder, Lang & Buchner, 2007).

Results

The mean CF-ED for the medial and lateral sides of the 4 tissues are presented in Table 1. We found a significantly smaller diameter CFs on the medial side in each of the four cases compared to fibrils on the lateral side. The frequency histogram of CFs on the medial and lateral sides for each of the four cases/tissues are presented in Figure 2. The differences in CFs across the two sides, averaged across the four cases, were significant, with medial side showing smaller CFs (45.69 ± 7.89 nm) than the lateral side (54.18 ± 7.62 nm); $p<0.001$ (Table 1). The transmission electron micrographs of medial and lateral CFs were digitized and color coded to estimate distribution of CF-ED (Figure 3). The pattern of CF-ED distribution is shown in an overall frequency histogram (Figure 4), and percentage of CF-ED falling in different range is presented in Table 2.

For the medial side, we found that the percentage of CF-ED were almost equally in the 29-44 nm and 45-59 nm ranges. Whereas, the lateral side CF-ED showed a wide-range, with majority (70%) of CF-ED falling within 45-59 nm (Table 2). We further calculated collagen fibril number density (CF-ND) and total cross-sectional area fraction of the CFs as a valuable indicator to determine the packing of the CFs. We found a higher CF-ND for the medial tissue (538) compared to the lateral tissue (376). The calculated averaged FAF showed a higher percentage value of 32.28 ± 8.13% for the medial side and a smaller percentage value of 27.28 ± 3.77% for the lateral side (Table 3, Figure 3).

Discussion

In the present preliminary study we demonstrate for the first time an estimation of CFs in the medial and lateral aspects of upper lip structure obtained from CL/P cases at primary lip surgery. We observed a significant difference in diameter of collagen fibril (CF-ED) between medial and lateral sides of CL. The collagen fibril density (CF-ND) was found to be higher for the medial side. Estimation of collagen fibril-area fraction (FAF) showed a higher percentage value for the medial side compared to lateral side.

We observed a significant difference ($p<0.001$) in CF-ED between medial (45.69 ± 7.89 nm) and lateral (54.18 ± 7.62 nm) CL tissues, with the medial tissue having a smaller CF-ED compared to lateral tissue. This observation of mean difference across the two tissues appears to be compatible with the finding of Moeller et al., (1995) that mechanical overloading on the connective tissue could eventually cause the thick CFs to become thinner. Based on this finding, we infer that mechanical stimuli may affect CF-ED distribution across the two cleft sides, reflected in the observed differences (Table 2; Figure 4).

Estimation of CF-ND and FAF provided valuable indication on how tightly or loosely packed is the CFs across the two sides of CL. The CF-ND or number of collagen fibrils per micrometer square area was found to be higher for the medial side compared to the lateral side (Table 3). This arrangement may reflect an increased mechanical load distribution across the two sides, with medial side showing higher value for CF-ND. Moreover, our result showed that despite having a smaller CF-ED, increasing CF-ND resulted in an increased FAF (32.28 ± 8.13%) for the medial side compared to lateral side (27.28 ± 3.77%), clearly represented in color coded image (Figure 3e & 3f). This indicates that medial side gains strength and stiffness with increase in FAF, which adds to the mechanical load of the medial tissues.

Studies elsewhere have shown that small and large fibrils have distinct roles in stiff state and only the small fibrils have a role in the disease states and hence lending to changing properties (Goh & Holmes, 2017), which could be the case in our medial tissues. Nonetheless, the possible role of factors apart from CF-ED or a consequence of CF-ED cannot be ruled out for compromised extracellular matrix of the medial tissue, based on previously described ability of metalloproteinases and their inhibitors to participate in matrix remodeling during lip fusion (Smane-Filipova et al., 2016). We postulate that remodeling of the extracellular matrix components (collagen fibers and/or proteoglycans) that forms the migration substrate for the cranial neural crest cells mesenchyme (Henderson & Copp, 1997; Jiang et al., 2006) could be different across the two sides. Some empirical evidence of reduced proliferation and migration of these mesenchymal cells particularly affected on the

medial side is shown in a separate animal study (Everson et al., 2017). Moreover, these mesenchymal cells eventually form the continuous bands of the future orbicularis oris muscle (Lazzeri et al., 2008), which is shown to have altered diameter (Khan et al., 2018) and arrangement (Wijayaweera, Amaratunga, & Angunawela, 2000) across the two sides in CL cases. Notably, collagen and muscles share structural functional relationship to ensure proper alignment (Calvi et al., 2012). Therefore, observation of changes in the orbicularis oris muscles across the two sides could be an outcome of changes in distribution of CF-ED, which affects the medial side more than the lateral side in cases with CL.

It is well known that the diameter of the CFs increase with age (Ottani et al., 1998). We consider that our observation of differences in CFs distribution across the two cleft sides is little influenced by ageing as we used tissues derived from the same individual with relatively similar age. However, we realize that inclusion of CL and CLP subtype might have influenced our result but relying on a recent study demonstrating similar rate of development of the two subtypes, the effect might have been neutralized (Sharp et al., 2017).

Moreover, our study has potential limitations with respect to small sample size with low statistical power owing to difficulties in collecting tissues (Stock et al., 2016), and therefore we were unable adequately to assess inter-individual variability. We also note that lack of clarity or darker patches in our original image could have interfered in the binary image creation, leaving holes that might have affect on the measured parameters. Therefore, the differences in CFs across the two sides should be interpreted with caution until replication data become available; these would be based on a larger sample size and good quality input images for better segmentation of CFs while processing to binary images. Another limitation is the lack of data on lip tissues from normal babies to determine whether the difference between the sides is present in general population or is specific to infants with clefts. Nevertheless, investigation of differences using tissues from CL/P cases is a promising approach in investigating the etiopathology of CL/P.

In conclusion, the result of this study suggest of differences in CF-ED across the two cleft side, with medial side having smaller diameter and higher stiffness that might play a role in migration of mesenchymal cells in these tissues, causing a tissue deficiency that prevents contact with opposing lateral tissues, resulting in cleft lip. Additionally, our study could provide knowledge towards underlying tissue biomechanics that may help reconstruction of perioral tissue scaffolds, ultimately resulting in better treatment of patients with oral clefts.

Acknowledgements

We acknowledge the support received from the Department of Biomedical and Specialty Surgical Sciences, Section of Medical Biochemistry, Molecular Biology and Genetics, University of Ferrara, Italy (MFJK, postdoctoral fellowship, n. 62040 & 0039804). Further our sincere thanks to Dr. Houda Oudouche, Department of Humanities, University of Ferrara, Italy and Lab. Group members: Amin Ravaei, Valentina Aleotti, Luca Dall'Olio, Ilaria Cestonaro, Simone Ravalli, Giorgia Casagrande, Vincenzo Aiello and Gianni Astolfi for their assistance. JL holds a tier 1 Canada Research Chair.

Author contributions

MFJK designed the study, carried out experiment and drafted the manuscript. MR, LA and MCM managed recruitment of PENTACLEFT lip tissue samples. The data was analyzed by MFJK together with MR. MR, JL, PM, TCN and AM checked and revised the manuscript. MFJK and AS captured images on TEM. All authors read and approved the final manuscript.

Conflicts of interest

None to declare.

References

Dixon, M. J., Marazita, M. L., Beaty, T. H., & Murray, J. C. (2011). Cleft lip and palate: understanding genetic and environmental influences. *Nat Rev Genet*, 12(3), 167-178. doi: 10.1038/nrg2933

Leslie, E. J., Carlson, J. C., Cooper, M. E., Christensen, K., Weinberg, S. M., & Marazita, M. L. (2017). Exploring Subclinical Phenotypic Features in Twin Pairs Discordant for Cleft Lip and Palate. *Cleft Palate Craniofac J*, 54(1), 90-93. doi: 10.1597/15-190

Barlow, S. M., Trotman, C. A., Chu, S. Y., & Lee, J. (2012). Modification of perioral stiffness in patients with repaired cleft lip and palate. *Cleft Palate Craniofac J*, 49(5), 524-529. doi: 10.1597/10-092

Trotman, C. A., Barlow, S. M., & Faraway, J. J. (2007). Functional outcomes of cleft lip surgery. Part III: Measurement of lip forces. *Cleft Palate Craniofac J*, 44(6), 617-623. doi: 10.1597/06-138.1

Carroll, K., & Mossey, P. A. (2012). Anatomical variations in clefts of the lip with or without cleft palate. *Plast Surg Int*, 2012, 542078. https://doi.org/10.1155/2012/542078

Mossey, P. A., Little, J., Munger, R. G., Dixon, M. J., & Shaw, W. C. (2009). Cleft lip and palate. *Lancet*, 374(9703), 1773-1785. doi: 10.1016/S0140-6736(09)60695-4

Jiang, R., Bush, J. O., & Lidral, A. C. (2006). Development of the upper lip: morphogenetic and molecular mechanisms. *Dev Dyn*, 235(5), 1152-1166. doi: 10.1002/dvdy.20646

Walker, N. J., & Podda, S. (2018). *Cleft Lip* StatPearls. Treasure Island (FL).

McDaniel, D. P., Shaw, G. A., Elliott, J. T., Bhadriraju, K., Meuse, C., Chung, K. H., & Plant, A. L. (2007). The stiffness of collagen fibrils influences vascular smooth muscle cell phenotype. *Biophys J*, 92(5), 1759-1769. doi: 10.1529/biophysj.106.089003

Gagliano, N., Carinci, F., Moscheni, C., Torri, C., Pezzetti, F., Scapoli, L., . . . Stabellini, G. (2010). New insights in collagen turnover in orofacial cleft patients. *Cleft Palate Craniofac J*, 47(4), 393-399. doi: 10.1597/07-196.1

Badylak, S. F. (2005). Regenerative medicine and developmental biology: the role of the extracellular matrix. *Anat Rec B New Anat*, 287(1), 36-41. doi: 10.1002/ar.b.20081

Smane-Filipova, L., Pilmane, M., & Akota, I. (2016). MMPs and TIMPs expression in facial tissue of children with cleft lip and palate. *Biomed Pap Med Fac Univ Palacky Olomouc Czech Repub*, 160(4), 538-542. doi: 10.5507/bp.2016.055

Mansell, J. P., Kerrigan, J., McGill, J., Bailey, J., TeKoppele, J., & Sandy, J. R. (2000). Temporal changes in collagen composition and metabolism during rodent palatogenesis. *Mech Ageing Dev*, 119(1-2), 49-62.

Bosi, G., Evangelisti, R., Valeno, V., Carinci, F., Pezzetti, F., Calastrini, C., . . . Carinci, P. (1998). Diphenylhydantoin affects glycosaminoglycans and collagen production by human fibroblasts from cleft palate patients. *J Dent Res*, 77(8), 1613-1621. doi: 10.1177/00220345980770080901

Bodo, M., Baroni, T., Carinci, F., Becchetti, E., Bellucci, C., Pezzetti, F., . . . Carinci, P. (1999). TGFbeta isoforms and decorin gene expression are modified in fibroblasts obtained from non-syndromic cleft lip and palate subjects. *J Dent Res*, 78(12), 1783-1790. doi: 10.1177/00220345990780120401

Nagase, H., Visse, R., & Murphy, G. (2006). Structure and function of matrix metalloproteinases and TIMPs. *Cardiovasc Res*, 69(3), 562-573. doi: 10.1016/j.cardiores.2005.12.002

Levine, M. (2011). *The Connective Tissue Extracellular Matrix and Its Major Components*. In: Topics in Dental Biochemistry. Springer, Berlin, Heidelberg

Arseni, L., Lombardi, A., & Orioli, D. (2018). From Structure to Phenotype: Impact of Collagen Alterations on Human Health. *Int J Mol Sci*, 19(5). doi: 10.3390/ijms19051407

Chavrier, C., Couble, M. L., Magloire, H., & Grimaud, J. A. (1984). Connective tissue organization of healthy human gingiva. Ultrastructural localization of collagen types I-III-IV. *J Periodontal Res*, 19(3), 221-229.

Pego, S. P., de Faria, P. R., Santos, L. A., Coletta, R. D., de Aquino, S. N., & Martelli-Junior, H. (2016). Ultrastructural evaluation of gingival connective tissue in hereditary gingival fibromatosis. *Oral Surg Oral Med Oral Pathol Oral Radiol*, 122(1), 81-88 e82. doi: 10.1016/j.oooo.2016.04.002

Agrawal, U., Rai, H., & Jain, A. K. (2011). Morphological and ultrastructural characteristics of extracellular matrix changes in oral squamous cell carcinoma. *Indian J Dent Res*, 22(1), 16-21. doi: 10.4103/0970-9290.79968

Craig, A. S., Birtles, M. J., Conway, J. F., & Parry, D. A. (1989). An estimate of the mean length of collagen fibrils in rat tail-tendon as a function of age. *Connect Tissue Res*, 19(1), 51-62.

Craig, A. S., Eikenberry, E. F., & Parry, D. A. (1987). Ultrastructural organization of skin: classification on the basis of mechanical role. *Connect Tissue Res*, 16(3), 213-223.

Xu, L. X., Ohsaki, Y., Nagata, K., & Kurisu, K. (1993). Immunohistochemical studies on the distributions and age-related changes of types I and III collagen in the oral mucosa of mice. *J Dent Res*, 72(9), 1336-1343. doi: 10.1177/00220345930720091401

Brinkley, L. L., & Morris-Wiman, J. (1987a). Effects of chlorcyclizine-induced glycosaminoglycan alterations on patterns of hyaluronate distribution during morphogenesis of the mouse secondary palate. *Development*, 100(4), 637-640.

Brinkley, L. L., & Morris-Wiman, J. (1987b). Computer-assisted analysis of hyaluronate distribution during morphogenesis of the mouse secondary palate. *Development*, 100(4), 629-635.

Cornelissen, A. M., Stoop, R., Von den Hoff, H. W., Maltha, J. C., & Kuijpers-Jagtman, A. M. (2000). Myofibroblasts and matrix components in healing palatal wounds in the rat. *J Oral Pathol Med*, 29(1), 1-7.

Parry, D. A., Barnes, G. R., & Craig, A. S. (1978). A comparison of the size distribution of collagen fibrils in connective tissues as a function of age and a possible relation between fibril size distribution and mechanical properties. *Proc R Soc Lond B Biol Sci*, 203(1152), 305-321.

Parry, D. A. (1988). The molecular and fibrillar structure of collagen and its relationship to the mechanical properties of connective tissue. *Biophys Chem*, 29(1-2), 195-209.

Williams, L. N., Elder, S. H., Horstemeyer, M. F., & Harbarger, D. (2008). Variation of diameter distribution, number density, and area fraction of fibrils within five areas of the rabbit patellar tendon. *Ann Anat*, 190(5), 442-451. doi: 10.1016/j.aanat.2008.05.003

Robinson, P. S., Lin, T. W., Jawad, A. F., Iozzo, R. V., & Soslowsky, L. J. (2004). Investigating tendon fascicle structure-function relationships in a transgenic-age mouse model using multiple regression models. *Ann Biomed Eng*, 32(7), 924-931.

Herchenhan, A., Uhlenbrock, F., Eliasson, P., Weis, M., Eyre, D., Kadler, K. E., . . . Kjaer, M. (2015). Lysyl Oxidase Activity Is Required for Ordered Collagen Fibrillogenesis by Tendon Cells. *J Biol Chem*, 290(26), 16440-16450. doi: 10.1074/jbc.M115.641670

Zhang, J., Yang, R., Liu, Z., Hou, C., Zong, W., Zhang, A., . . . Gao, J. (2015). Loss of lysyl oxidase-like 3 causes cleft palate and spinal deformity in mice. *Hum Mol Genet*, 24(21), 6174-6185. doi: 10.1093/hmg/ddv333

Khan, M. F. J., Little, J., Mossey, P. A., Steegers-Theunissen, R. P., Bonsi, M., Bassi Andreasi, R., & Rubini, M. (2018). Association between a common missense variant in lysyl oxidase like 3 (LOXL3) gene and the risk of non-syndromic cleft palate. *Congenit Anom*. doi: 10.1111/cga.12288

Meng, L., Bian, Z., Torensma, R., & Von den Hoff, J. W. (2009). Biological mechanisms in palatogenesis and cleft palate. *J Dent Res*, 88(1), 22-33. doi: 10.1177/0022034508327868

Khan, M. F. J., Little, J., Mossey, P. A., Steegers-Theunissen, R. P., Autelitano, L., Lombardo, I., . . . Rubini, M. (2018). Evaluating LINE-1 methylation in cleft lip tissues and its association with early pregnancy exposures. *Epigenomics*, 10(1), 105-113. doi: 10.2217/epi-2017-0081

Khan, M. F. J., Nag, T. C., Igathinathane, C., Osuagwu, U. L., & Rubini, M. (2015). A new method of detecting changes in corneal health in response to toxic insults. *Micron*, 78, 45-53. doi: 10.1016/j.micron.2015.07.007

Ferreira, T. (2014). *ROI Color Coder*. Ver. 5.1. ImageJ Documentation Wiki. http://imagejdocu.tudor.luFreund

Ferreira, T., & Rasband, W. (2012). *ImageJ user guide*, IJ 1.46r. https:// imagej.nih.gov/ij/docs/guide/user-guide.pdf

Starborg, T., Kalson, N. S., Lu, Y., Mironov, A., Cootes, T. F., Holmes, D. F., & Kadler, K. E. (2013). Using transmission electron microscopy and 3View to determine collagen fibril size and three-dimensional organization. *Nat Protoc*, 8(7), 1433-1448. doi: 10.1038/nprot.2013.086

Faul F, Erdfelder E, Lang AG and Buchner A (2007). G*Power 3: a flexible statistical power analysis program for the social, behavioral, and biomedical sciences. *Behavior research methods* 39: 175-91.

Moeller, H. D., Bosch, U., & Decker, B. (1995). Collagen fibril diameter distribution in patellar tendon autografts after posterior cruciate ligament reconstruction in sheep: changes over time. *J Anat*, 187 (Pt 1), 161-167.

Goh, K. L., & Holmes, D. F. (2017). Collagenous Extracellular Matrix Biomaterials for Tissue Engineering: Lessons from the Common Sea Urchin Tissue. *Int J Mol Sci*, 18(5). doi: 10.3390/ijms18050901

Henderson, D. J., & Copp, A. J. (1997). Role of the extracellular matrix in neural crest cell migration. *J Anat*, 191 (Pt 4), 507-515.

Everson, J. L., Fink, D. M., Yoon, J. W., Leslie, E. J., Kietzman, H. W., Ansen-Wilson, L. J., . . . Lipinski, R. J. (2017). Sonic Hedgehog regulation of Foxf2 promotes cranial neural crest mesenchyme proliferation and is disrupted in cleft lip morphogenesis. *Development*. doi: 10.1242/dev.149930

Lazzeri, D., Viacava, P., Pollina, L. E., Sansevero, S., Lorenzetti, F., Balmelli, B., . . . Massei, A. (2008). Dystrophic-like alterations characterize orbicularis oris and palatopharyngeal muscles in patients affected by cleft lip and palate. *Cleft Palate Craniofac J*, 45(6), 587-591. doi: 10.1597/07-026.1

Khan, M. F. J., Little, J., Abelli, L., Mossey, P. A., Autelitano, L., Nag, T. C., & Rubini, M. (2018). Muscle fiber diameter assessment in cleft lip using image processing. *Oral Dis*, 24(3), 476-481. doi: 10.1111/odi.12790

Wijayaweera, C. J., Amaratunga, N. A., & Angunawela, P. (2000). Arrangement of the orbicularis oris muscle in different types of cleft lips. *Journal of Craniofacial Surgery*, 11(3), 232–235.

Calvi, E. N., Nahas, F. X., Barbosa, M. V., Calil, J. A., Ihara, S. S., Silva Mde, S., . . . Ferreira, L. M. (2012). An experimental model for the study of collagen fibers in skeletal muscle. *Acta Cir Bras*, 27(10), 681-686.

Ottani, V., Franchi, M., De Pasquale, V., Leonardi, L., Morocutti, M., & Ruggeri, A. (1998). Collagen fibril arrangement and size distribution in monkey oral mucosa. *J Anat*, 192 (Pt 3), 321-328.

Sharp, G. C., Ho, K., Davies, A., Stergiakouli, E., Humphries, K., McArdle, W., . . . Relton, C. L. (2017). Distinct DNA methylation profiles in subtypes of orofacial cleft. *Clin Epigenetics*, 9, 63. doi: 10.1186/s13148-017-0362-2

Stock, N. M., Humphries, K., Pourcain, B. S., Bailey, M., Persson, M., Ho, K. M., . . . Sandy, J. (2016). Opportunities and Challenges in Establishing a Cohort Study: An Example From Cleft Lip/Palate Research in the United Kingdom. *Cleft Palate Craniofac J*, 53(3), 317-325. doi: 10.1597/14-306

Table 1. Mean ± Standard deviation (SD) values of collagen fibril edge diameter (CF-ED in nm) on the medial and lateral sides of four N1-N4 (number of measured CFs) infants with cleft lip.

Cleft lip tissues	**N1** (532)	**N2** (289)	**N3** (509)	**N4** (511)	**Mean N1-N4** (1841)
Medial	36.32 ± 4.21	47.99 ± 6.03	46.85 ± 4.31	52.98 ± 4.21	45.69 ± 7.89
Lateral	51.74 ± 7.04	49.63 ± 5.36	58.73 ± 7.82	54.76 ± 6.57	54.18 ± 7.62
	Z= -19.637 p<0.001	Z= -2.774 p=0.006	Z= -18.568 p<0.001	Z= -5.792 p<0.001	Z= -28.387 p<0.001

Table 2. Percentages of collagen fibril-edge diameters (CF-ED) in different ranges on the medial and lateral sides of the cleft lip in four affected infants.

Cleft lip tissues	**15-29 nm**	**30-44 nm**	**45-59 nm**	**60+ nm**
Medial	2	40	57	1
Lateral	<1	10	70	19

Table 3. Collagen number density (CF-ND) and fibril area fraction (FAF) on the medial and lateral sides of the cleft lip in four affected infants.

Cleft lip tissues	**Density of collagen fibrils** (μ^2)	**Area fraction of collagen fibrils** (%)
Medial	538	32.28 ± 8.13
Lateral	376	27.28 ± 3.77
	p=0.477	p=0.415

Figure 1. **Preprocessing of micrographs using ImageJ standard commands to obtain digital color-coded image.** (a) original 8-bit grey-scale image; (b) thresholding image with "moments" scheme and "no dark background" to convert image to binary format; (c) mask prepared by analyzing the particles with "no exclude edge" and "fill holes" options; (d) inverted mask giving black background using "invert"; and (e) "watershed" segmented image; (f) labelled collagen bundles; and (g) area based color-coded collagen bundles for better visualization of sizes.

Figure 2. **Frequency histogram of collagen fibril diameter (CF-ED) for medial and lateral cleft sides of each of the four cases (**N1, N2, N3 & N4**).**

Figure 3. **Electron micrograph, binary images and digital images of collagen fibrils of the medial and lateral sides of CL.** (a) original grey-scale image of medial side with smaller CF-ED; (b) original grey-scale image of the lateral side larger CF-ED; (c) binary image of medial and (d) lateral side; (e) digital colour coded image of medial side with higher CF-ND and FAF; (f) lateral side showing smaller CF-ND and smaller FAF.

Figure 4. **Overall (**N1-N4**) frequency histogram of collagen fibril diameter (CF-ED) for medial and lateral cleft sides.**

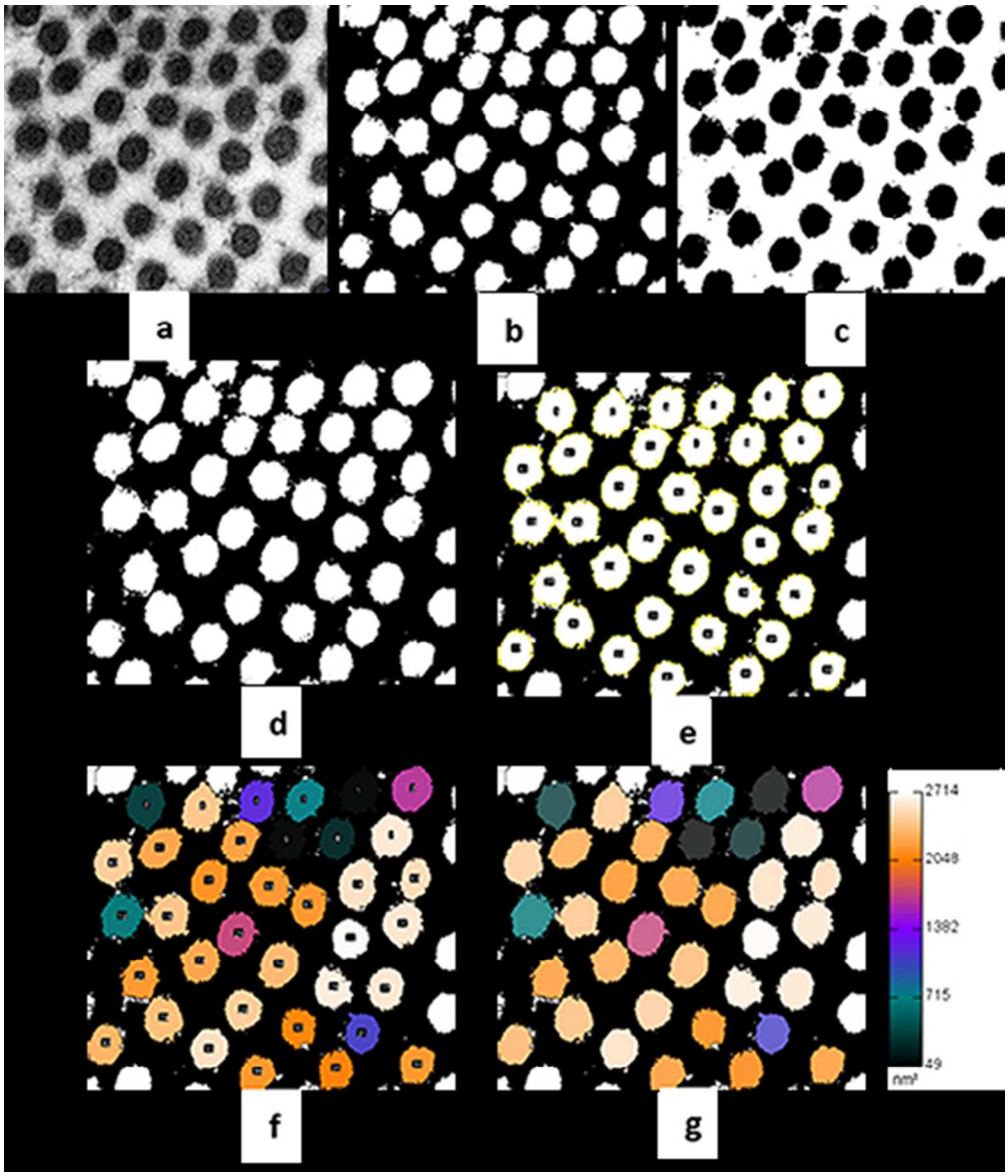

Preprocessing of micrographs using ImageJ standard commands to obtain digital color-coded image. (a) original 8-bit grey-scale image; (b) thresholding image with "moments" scheme and "no dark background" to convert image to binary format; (c) mask prepared by analyzing the particles with "no exclude edge" and "fill holes" options; (d) inverted mask giving black background using "invert"; and (e) "watershed" segmented image; (f) labelled collagen bundles; and (g) area based color-coded collagen bundles for better visualization of sizes.

176x205mm (72 x 72 DPI)

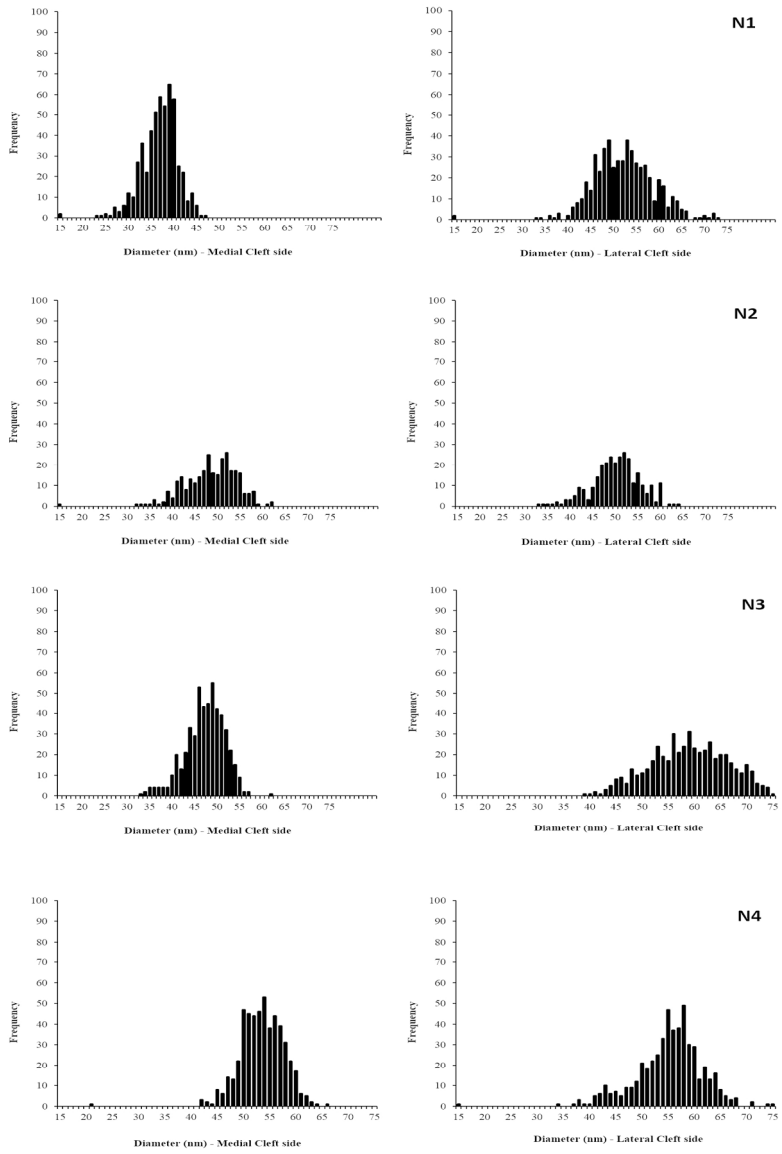

Frequency histogram of collagen fibril diameter (CF-ED) for medial and lateral cleft sides of each of the four cases (N1, N2, N3 & N4).

336x481mm (150 x 150 DPI)

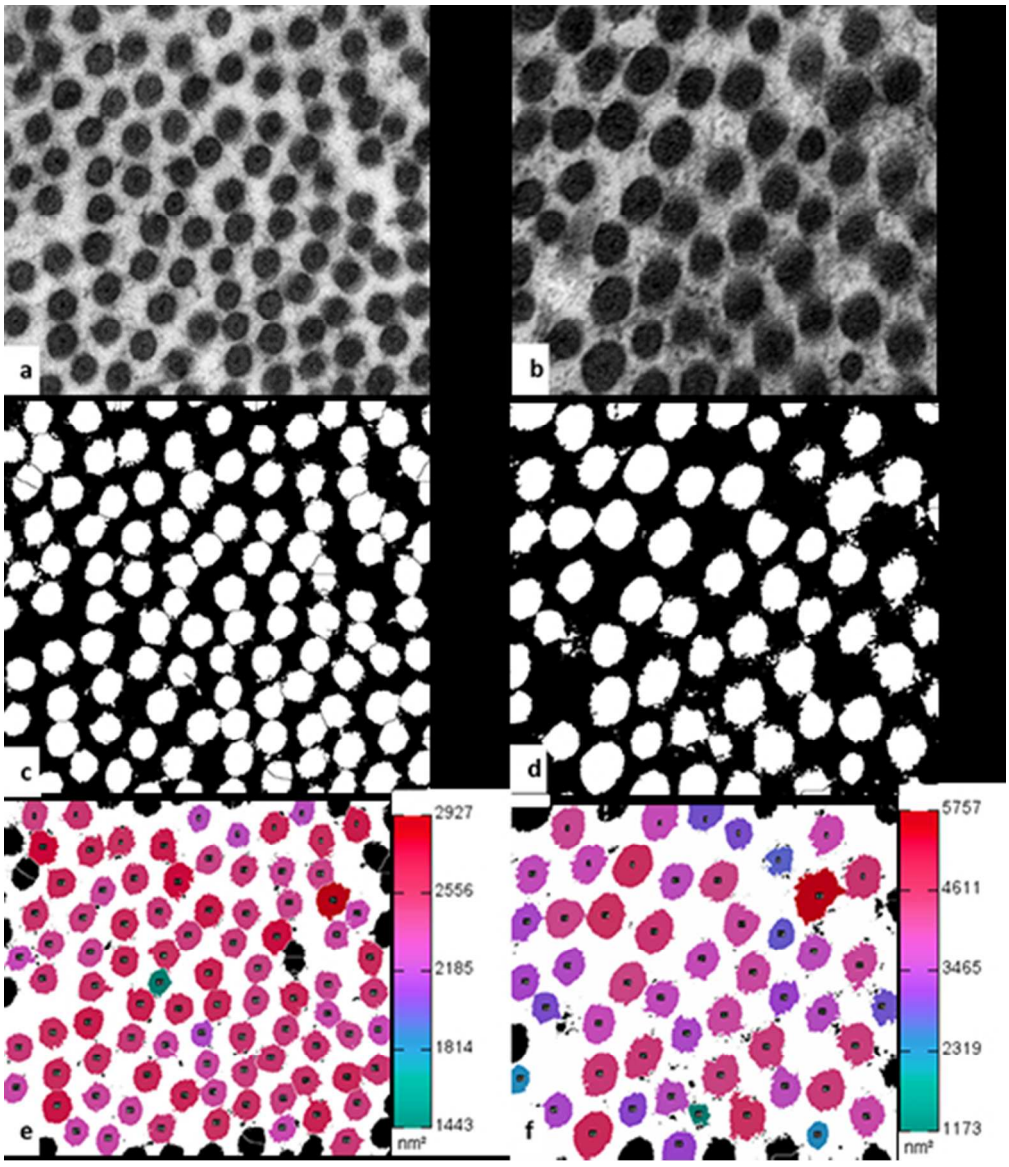

Electron micrograph, binary images and digital images of collagen fibrils of the medial and lateral sides of CL. (a) original grey-scale image of medial side with smaller CF-ED; (b) original grey-scale image of the lateral side larger CF-ED; (c) binary image of medial and (d) lateral side; (e) digital colour coded image of medial side with higher CF-ND and FAF; (f) lateral side showing smaller CF-ND and smaller FAF.

167x192mm (76 x 76 DPI)

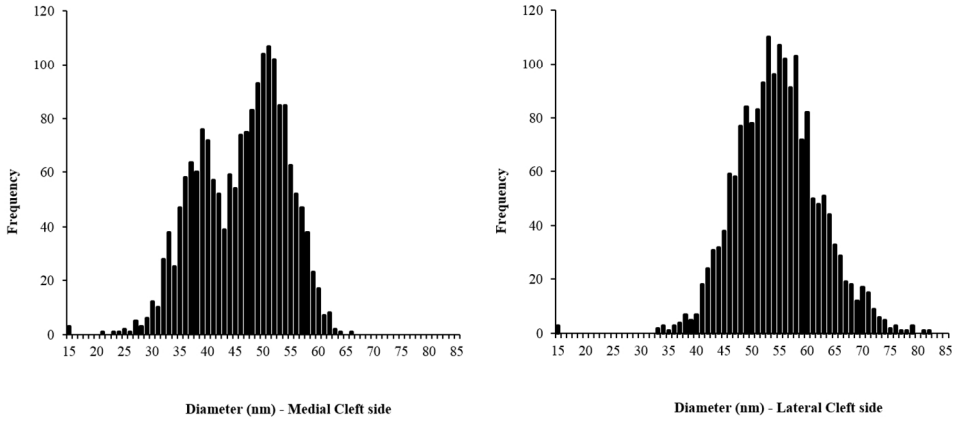

Overall (N1-N4) frequency histogram of collagen fibril diameter (CF-ED) for medial and lateral cleft sides.

248x121mm (150 x 150 DPI)